*2005 International Nuclear Atlantic Conference - INAC 2005*
*Santos, SP, Brazil, August 28 to September 2, 2005*

# SIMULATION OF IRIS PRESSURIZER OUT-SURGE TRANSIENT USING TWO AND THREE VOLUMES SIMULATION MODELS

**David A. Botelho, Paulo A. B. De Sampaio, and Maria de Lourdes Moreira,**
***Instituto de Engenharia Nuclear, Rio de Janeiro***

**Antônio Carlos de O. Barroso,** ***IPEN, São Paulo***

## ABSTRACT

Numeric models of the IRIS reactor pressurizer having either two or three volumes were employed to simulate a typical out-surge transient. The vapor volume may contain liquid drops. Vapor bubbles can be generated in the liquid volume. The mass, the energy, the constitutive, and the state equations, represent all relevant phenomena. A pressure equation is derived by the substitution of the mass and energy equations onto the presurizer volume constraint, assuming that the instantaneous pressure is the same in all volumes. The pressurizer experimental data of a loss of load transient in the Shippingport reactor is used to validate these pressurizer models. These models are also employed to verify the capacity of the thermal power controller to restore the pressure in the IRIS out-surge transient. The preliminary validation, using the Shippingport experimental data, and the close agreement reached by all the developed software, for the IRIS out-surge transient, recommends further validation of these models for the test evaluation and the design of scaled experiments for the IRIS pressurizer.

## 1. INTRODUCTION

The IRIS reactor, steam generator and primary pumps are contained within an integral vessel. The pressurizer is contained within the integral vessel upper head. It has a larger steam volume for the reactor core power than the current PWRs. Because of its large volume, the IRIS pressurizer does not need a spray system of sub-cooled liquid to reduce pressure increments due to in-surge transients, but heaters are provided in the lowest liquid volume. The lowest liquid volume of the pressurizer is separated from the circulating reactor coolant by a dividing steel structure that contains the surge flow path. Part of the pressurizer test scope is the simulation of surges in and out of the pressurizer, and the simulation of the heater operating modes.

## 2. MASS AND ENERGY CONSERVATION EQUATIONS

The three-volume model consists of an upper volume of vapor, an intermediate volume of liquid situated in part of the hemispheric volume, and a fixed volume of liquid located in a cylinder below the pressurizer hemisphere. In the two-volume model, the liquid volumes are collapsed in one volume that spreads from part of the liquid hemispheric volume to the liquid in the lower cylinder. The mass conservation equations are written in terms of the mass flow rates crossing internal interfaces and the surge interface. The internal energy conservation equations are written in terms of the convective heat rate, the thermal power, and the mechanical power [1]. The mechanical power is defined as the pressure times the volume rates. The mass conservation equations for the vapor, the upper liquid, and the lower liquid of the pressurizer are:

$$\frac{d}{dt}\left(m_v\right)=W_{FL_1}-W_{RO}-W_{WC}-\dot{m}_{l_1v} \tag{1}$$

$$\frac{d}{dt}\left(m_{l_1}\right)=W_{FL_2}-W_{FL_1}+W_{RO}+W_{WC}+\dot{m}_{l_1l_2}+\dot{m}_{l_1v} \tag{2}$$

$$\frac{d}{dt}\left(m_{l_2}\right)=\dot{m}_{surge}-W_{FL_2}-\dot{m}_{l_1l_2} \tag{3}$$

The energy conservation equations for the vapor, the upper liquid, and the lower liquid of the pressurizer are:

$$\frac{d}{dt}\left(m_v h_v\right)=\left(W_{FL_1}-W_{WC}\right)h_g-W_{RO}h_f-\dot{Q}_{l_1v}-\dot{Q}_{wv}-\dot{m}_{l_1v}h_{l_1v}+\left(m_v v_v\right)\frac{dp}{dt} \tag{4}$$

$$\begin{aligned}\frac{d}{dt}\left(m_{l_1}h_{l_1}\right)=&\left(W_{RO}+W_{WC}\right)h_f+\left(W_{FL_2}-W_{FL_1}\right)h_g+\left(m_{l_1}v_{l_1}\right)\frac{dp}{dt}\\&+\dot{Q}_{l_1v}+\dot{m}_{l_1v}h_{l_1v}-\dot{Q}_{l_1l_2}-\dot{Q}_{wl_1}+\dot{m}_{l_1l_2}h_{l_1l_2}\end{aligned} \tag{5}$$

$$\frac{d}{dt}\left(m_{l_2}h_{l_2}\right)=\dot{m}_{surge}h_{surge}-W_{FL_2}h_g+\dot{Q}_{l_1l_2}-\dot{Q}_{wl_2}-\dot{m}_{l_1l_2}h_{l_1l_2}+\dot{Q}_{heater}+\left(m_{l_2}v_{l_2}\right)\frac{dp}{dt} \tag{6}$$

In the three-volume model, the lower liquid volume is fixed. This constraint condition is used to calculate the mass flow rate on the interface between the two liquid volumes. The mass flow rate equation is derived by the substitution of the mass balance equation of the lower liquid volume into the volume constraint condition. The final result is [2,3]

$$\dot{m}_{l_1l_2}^{(t+\Delta t)}=\dot{m}_{surge}^{(t+\Delta t)}-W_{FL_2}^{(t+\Delta t)}+\frac{\left(m_{l_2}^{(t)}\right)^2}{Vol_{l_2}}\left[\left(\frac{\partial v_{l_2}}{\partial h_{l_2}}\right)_p\frac{h_{l_2}^{(t)}-h_{l_2}^{(t-\Delta t)}}{\Delta t}+\left(\frac{\partial v_{l_2}}{\partial p}\right)_{h_{l_2}}\frac{p^{(t)}-p^{(t-\Delta t)}}{\Delta t}\right] \tag{7}$$

The total volume of the pressurizer is also invariant with time. As the lower liquid volume is fixed, the remaining volume constraint condition is used to derive the following pressure equation

$$v_v\frac{dm_v}{dt}+v_{l_1}\frac{dm_{l_1}}{dt}+\left(\frac{\partial v_v}{\partial h_v}\right)_p m_v\frac{dh_v}{dt}+\left(\frac{\partial v_{l_1}}{\partial h_{l_1}}\right)_p m_{l_1}\frac{dh_{l_1}}{dt}+\left[m_{l_1}\left(\frac{\partial v_{l_1}}{\partial p}\right)_{h_{l_1}}+m_v\left(\frac{\partial v_v}{\partial p}\right)_{h_v}\right]\frac{dp}{dt}=0 \tag{8}$$

The substitution of the vapor and the upper liquid volume mass balance equations and energy balance equations into Eq. (8) finalizes the derivation of the pressure differential equation. Closure constitutive relations define the unknown mass flow rates. Liquid and steam thermodynamic state equations are also used for closure.

## 3. CONSTITUTIVE MODELS

The heat diffusion from the lower liquid volume to the middle liquid volume is neglected. The mass exchange on the interface of the vapor volume and the middle liquid volume is calculated using the gas kinetic theory. The heat exchange on the interface of the vapor volume and the middle liquid volume is calculated using a convective heat transfer coefficient [4].

Liquid drops are generated in the vapor volume due to bulk condensation (rainout) [5, 6]. Due to the large density of a liquid drop as compared to the density of the vapor volume, the drops never reach speeds needed for significant drag force. Thus the liquid drops reach the interface with the velocity of a free falling body. They enter the liquid volume through the liquid interface. The rainout mass flow rate is defined in terms of the interface area, the liquid fraction in the vapor volume, and the drop final velocity in the vapor volume.

Vapor bubbles are generated in the liquid volume due to bulk evaporation (flashing) [5, 6]. Due to the small density of the vapor bubble as compared to that of the liquid volume, the drops can have a significant (buoyancy minus gravity) acceleration. Thus they reach sufficient speed for significant drag force. The flashing mass flow rate is defined in terms of the interface area, the vapor fraction in the liquid volume, and bubble terminal velocity in the liquid volume, that is calculated using the Wilson formula [7]. The transient rainout and flashing mass flow rates are calculated employing a transit time delay model [6].

The mass flow rate due to vapor condensation on the wall in the vapor volume is calculated from the wall condensation equation derived from the mass and energy jump conditions on this interface [1]. The heat transfer coefficient for condensation is calculated using the model derived by Nusselt (shown in the reference [8]). The wall temperature can be calculated solving a wall conduction equation with a heat transfer coefficient averaged over all volumes.

## 4. HEATER SIMULATION CONTROL

The pressurizer heaters are simulated using a time delay equation with a typical time constant. Therefore, the equation for the time behavior of the pressurizer heaters is [5]

$$\frac{d\dot{Q}_{heater}}{dt} = \frac{1}{\tau_h}\left(\dot{Q}_{elect}^{(t)} - \dot{Q}_{heater}\right) \tag{9}$$

The proportional heater bank is controlled as [3]

$$\dot{Q}_{PI}^{(t)} = \left[K_p\left(\frac{p_{set}-p}{p_{set}}\right) + K_i\int_{t_0}^{t}\left(\frac{p_{set}-p}{p_{set}}\right)dt\right]\dot{Q}_{PI}^{Total} + \dot{Q}_{PI}^{(t_0)} \tag{10}$$

The proportional heater bank power is limited to the $\dot{Q}_{PI}^{Total}$ value. The back-up heater banks power is the design value when the pressure is within the interval of the prescribed pressure set points, and zero, when the pressure is outside this interval. The total electric power in the pressurizer electric heaters is the sum of the power of the proportional heater bank and the power of the back-up heater banks.

## 5. MODEL VALIDATION

This pressurizer model was compared to the experimental data of a 74 MW loss of load transient in the Shippingport reactor [6] using its heaters, spray, and relief valve specific controls. As is shown in Figure 1, the results for the three-volume and the two-volume models, using a separate solver, are almost identical. Both results show a very little discrepancy from results of the two-volume model using a simultaneous solver. Despite some uncertainty in the insurge and spray enthalpy, the numeric results from these models are considered in good agreement with the Shippingport pressurizer experimental data.

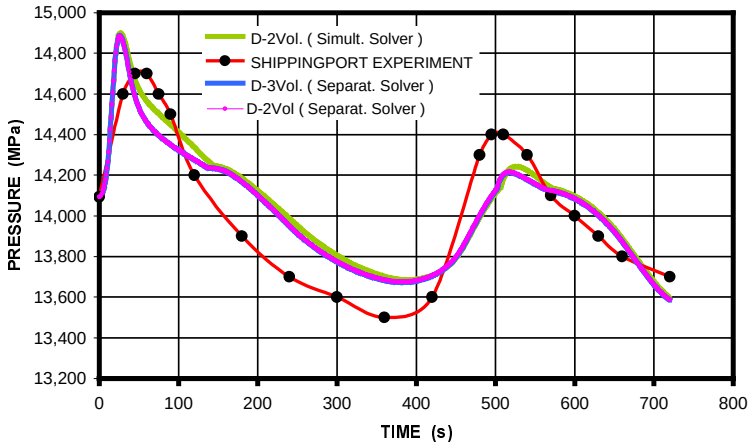


**Figure 1. Loss of load of the Shippingport reactor**

## 6. IRIS PRESSURIZER TRANSIENT SIMULATION

In IRIS, the pressurizer is located in the upper head of the integral vessel (for the reactor, steam generators, and main pumps), above the internal control rod mechanisms. This placement is considered optimal for the IRIS design, since it maximizes the overall pressurizer volume. The IRIS pressurizer layout is shown in the Fig. 2.

The three and the two volume models were used to simulate numerically a typical out-surge transient in the IRIS pressurizer. The driving parameter in this transient is the mass flow rate through the surge orifices, calculated in a primary circuit simulation [3]. The mass flow rate curve is shown in Fig. (3). In surge events, the pressure is controlled by the heater power. The heater power value calculated by the heater controller is shown in the Fig. 4. Using the various numerical models, the pressure curves are shown in the Fig. 5. Notice the pressure stabilization by the heater controller. The D-labeled results in the Fig. 4 and Fig. 5 have the wall condensation energy terms explicitly represented in the energy equations. In the B-labeled results the wall condensation is contained in the heat transfer coefficient to calculate the heat losses to the pressurizer wall. As shown in Figure 4, all results of the three-volume and the two-volume models are almost identical, using either a separate solver or a simultaneous solver. The B-labeled and the D-labeled software were developed independently, and a preliminary “validation” was performed for the D-labeled software.

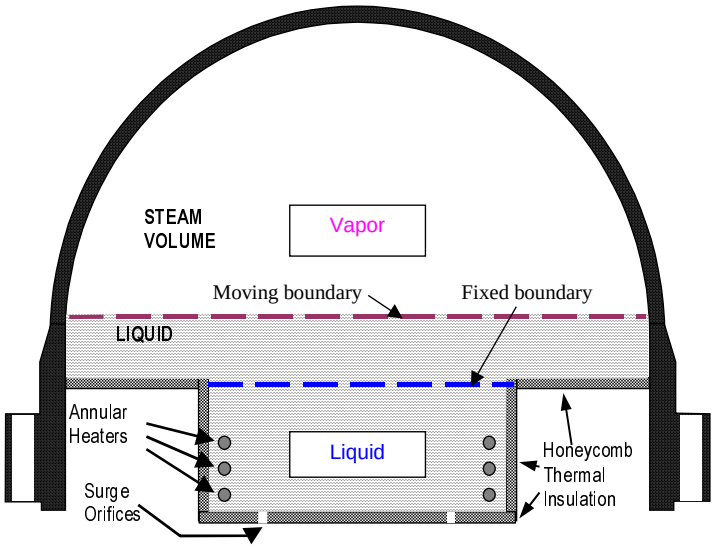


**Figure 2. The IRIS pressurizer layout**

The preliminary validation and the agreement of the curves demonstrate that the calculated pressure curves can correctly represent the response of the IRIS pressurizer to out-surge transients.

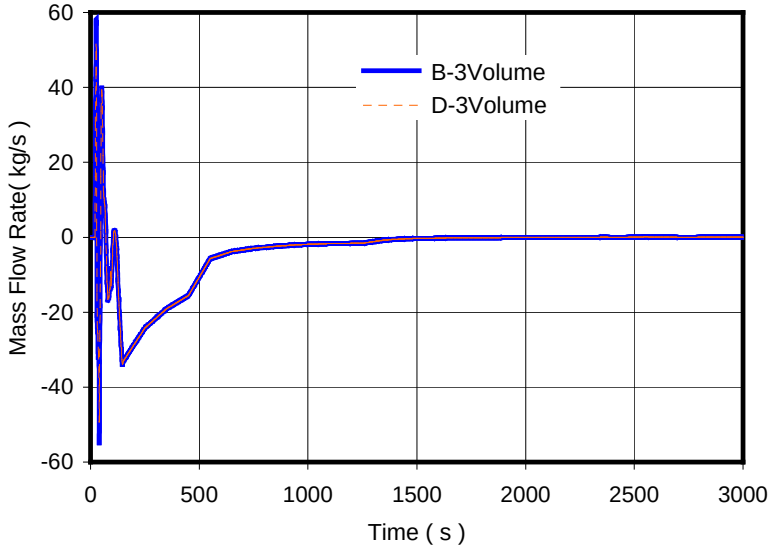


**Figure 3. Surge mass flow rate**

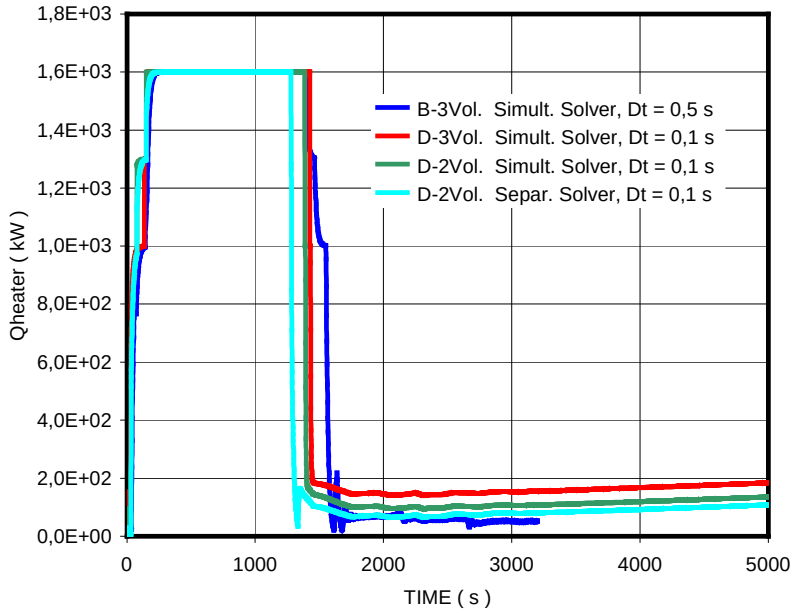


**Figure 4. The heater power control in the IRIS pressurizer**

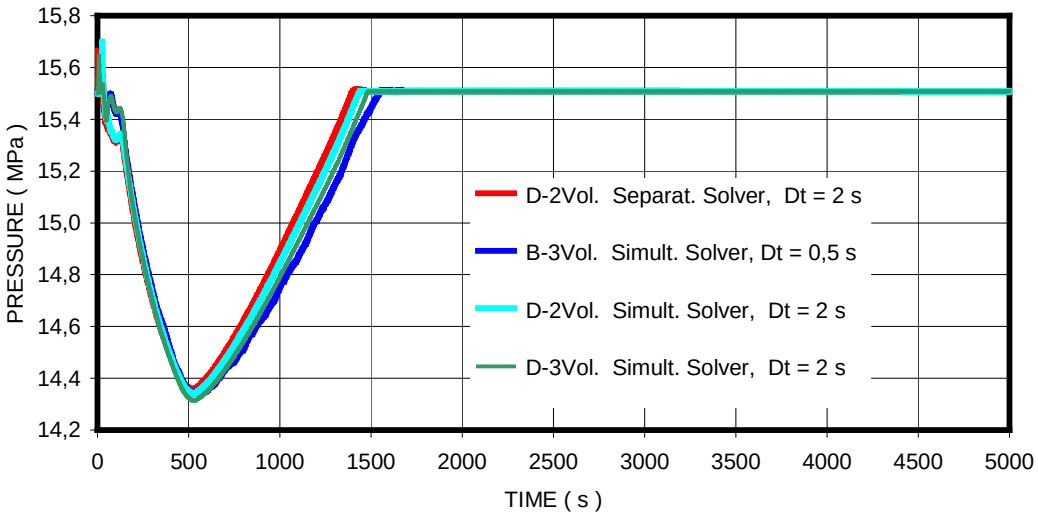


**Figure 5. The out-surge pressure transient in the IRIS pressurizer**

## 7. CONCLUSION

As shown, the results of the three-volume and the two-volume models are almost identical, using either a separate solver or a simultaneous solver. The preliminary validation, using the Shippingport experimental data, and the close agreement reached by all the developed software, for the IRIS out-surge transient, recommends further validation of these models for the test evaluation and the design of scaled experiments for the IRIS pressurizer.

## NOMENCLATURE

$h$ = Enthalpy per unit mass $m$ = Mass $\dot{m}, W$ = Mass flow rate $p$ = Pressure
$\dot{Q}$ = Thermal power $t$ = Time $v$ = Volume per unit mass $V$ = Volume

Subscripts: FL=Flashing, RO=Rain-out, WC=Wall condensation, PI=Proportional-integral, p=proportional, i=Integral, f=Saturated liquid g=Saturated vapor

## REFERENCES


1. N. E. Todreas and M. S. Kazimi, *Nuclear Systems I, Thermal Hydraulic Fundamentals*, Taylor & Francis, Levittown, USA (1990).
2. A. C. O. Barroso and B. D. Batista Fo., "Refining the Design of the IRIS Pressurizer," *Proceeding of the 5th International Conference on Nuclear Option in Countries with Small and Medium Electricity Grids*, Dubrovnik, Croatia (2004).
3. A. C. O. Barroso, B. D. Batista Fo., I. D. Arone, L. A. Macedo, P. A. B. Sampaio, and M. Morais, "IRIS Pressurizer Design," *Proceedings of the ICAPP*, Cordoba, Spain, Paper 3227 (2003).
4. S.-W. Kang and P. Griffith, "Pool Heat Transfer in a Simulated PWR Pressurizer," *Transactions of the ANS*, **Vol. 46**, pp. 845-847 (1984).
5. R. C. Baron, "Digital Model Simulation of a Nuclear Pressurizer**,"** *Nuclear Science and Engineering*, **Vol. 52**, pp. 283-291 (1973).
6. A. N. Nahavandi and S. Makkenchery, "An Improved Pressurizer Model with Bubble Rise and Condensate Drop Dynamics**,"** *Nuclear Engineering and Design*, **Vol. 12**, pp. 135-147 (1970).
7. J. F. Wilson, R. J. Grenda, and J. F. Patterson, "Steam Volume Fraction in a Bubbling Two-Phase Mixture," *Transactions of the American Nuclear Society*, **Vol. 4, section 37**, PP 356-357 (1961).
8. J. P. Holman, *Heat Transfer*, McGraw-Hill Book Company, Singapore (1989).